

# Dynamical excitations of one-dimensional Fulde-Ferrell pairing Fermi superfluid

Peng Zou<sup>1</sup>, Huaisong Zhao<sup>1,\*</sup>, Feng Yuan<sup>1</sup>, and Shi-Guo Peng<sup>2†</sup>

<sup>1</sup>*College of Physics, Qingdao University, Qingdao 266071, China and*

<sup>2</sup>*State Key Laboratory of Magnetic Resonance and Atomic and Molecular Physics, Innovation Academy for Precision Measurement Science and Technology, Chinese Academy of Sciences, Wuhan 430071, China*

We theoretically investigate a one-dimensional Fulde-Ferrell Fermi superfluid at a finite effective Zeeman field  $h$ , and study entire dynamical excitations related to density perturbation. By calculating the density dynamic structure factor, we find anisotropic dynamical excitations in both collective modes and single-particle excitations. Along the direction of centre-of-mass momentum  $p$ , there are two obvious gapless collective modes with different speed. The lower collective modes is from the usual gauge symmetry breaking and has a larger speed than the one in the negative direction of  $p$ . The higher one is due to the direction spontaneous symmetry breaking of centre-of-mass momentum  $p$ , and separates two kinds of single-particle excitations in the positive  $p$  direction. However, this higher mode disappears in the opposite direction of  $p$ , where two single-particle excitations overlap with each other. These signals of dynamical excitations can do help to distinguish Fulde-Ferrell superfluid from the conventional Bardeen-Cooper-Schrieffer superfluid in the future experiment.

## I. INTRODUCTION

Since the discovery of superconducting phenomena in mercury by K. Onnes in 1911, it is realized that particles with opposite momentum and spin can generate a molecular Cooper pair carrying zero center-of-mass (COM) momentum to decrease energy. This conventional Bardeen-Cooper-Schrieffer (BCS) superfluidity originates from the Bose-Einstein-Condensation (BEC) of Cooper pairs at zero momentum. Later it is theoretically predicted by Fulde and Ferrel [1] and Larkin and Ovchinnikov [2] that Cooper pairs can also carry a finite COM momentum, and condense at a nonzero momentum  $p$  with order parameter in either a plane-wave FF-type  $\Delta(\mathbf{r}) = \Delta e^{i\mathbf{p}\cdot\mathbf{r}}$  or a standing-wave LO-type  $\Delta(\mathbf{r}) = \Delta \cos(\mathbf{p}\cdot\mathbf{r})$ . In such an ansatz, the two mismatched Fermi surfaces of different spin components can overlap, thereby supporting a spatially inhomogeneous superfluidity. These pairing states generate an exotic Fulde-Ferrell-Larkin-Ovchinnikov (FFLO) superfluidity [3].

These FFLO superfluids have been actively searched for almost six decades. In condensed matter physics, some strong signals of FFLO states come from the research in heavy fermions [5–9] and organic superconductors [10], which are only indirect experimental evidences. Recently several experimental works reported evidence of pair-density-wave in high-Tc superconductor by scanning tunnelling microscopy technique [11–13], which ignites the passion again and provides new possibilities to search and study FFLO state. An ultracold atomic Fermi gas has proven to be an ideal tabletop system for the pursuit of FFLO superfluidity [14]. The FFLO state is thought to be very fragile in three dimensions and has quite narrow

parameter space. Both lower spatial dimension [15] and spin-orbit coupling effect [16, 17] in Fermi superfluid have been reported that they can expand the parameter space and theoretically investigate the possible phase diagrams related to FFLO state. Also a theoretical strategy via a Dark-State Control of Feshbach resonance was proposed to realize FF superfluid in ultracold atomic gases [18].

In fact it is expected that the full dynamical excitations of a certain matter state can be utilized to check the existence of this state, or distinguish it from other states. Dynamic structure factor is an important many-body physical quantity, and includes rich information related to dynamical excitations of the system [19, 20]. Experimentally dynamic structure factor can be directly measured by a two-photon Bragg scattering technique, which had been used to investigate dynamical excitations of the BCS-BEC crossover Fermi superfluid, including the single-particle excitations [21], collective Goldstone phonon mode [22], second sound [23] and Higgs mode [24]. A spin-charge separation of repulsive one-dimensional (1D) Fermi gas has also been studied by this technique [25]. Thus it is interesting to study the dynamical excitations of an FFLO Fermi superfluid, and find its dynamical characters related to its symmetry structure.

In this paper, we theoretically investigate a 1D spin-polarized Fermi superfluid in an FF-type pairing state, and discuss its entire dynamical excitations by numerically calculating the dynamic structure factor of this system with random phase approximation [26, 27]. We will initially discuss the state of equation of the system in FF superfluid, and then introduce all possible dynamical excitations, which may provide some background knowledge to anisotropic Josephson effect related to FFLO state. This paper is organized as follows. In the next section, we use the motion equation of Green's function to introduce the microscopic model of a 1D spin-polarized interacting Fermi gas, and outline the mean-field approximation, and then show how to calculate the response function with random phase approximation. We give re-

\* hszhao@qdu.edu.cn

† pengshiguo@wipm.ac.cn

sults of the dynamic structure factor of FF superfluids in Sec. III, and we give our conclusions and outlook in Sec. IV. Some calculation details are listed in the Appendix.

## II. METHODS

### A. Model and Hamiltonian

We consider a uniform 1D spin-polarized Fermi gases with s-wave contact interaction. The system can be described by a model Hamiltonian

$$H = \sum_{k\sigma} (\epsilon_k - \mu_\sigma) c_{k\sigma}^\dagger c_{k\sigma} + g_{1D} \sum_{pkk'} c_{k\uparrow}^\dagger c_{p-k\downarrow}^\dagger c_{p-k'\downarrow} c_{k'\uparrow}, \quad (1)$$

here  $\epsilon_k = k^2/2m$  is the dispersion relation of spin- $\sigma$  free particles with mass  $m$  in reference to the chemical potential  $\mu_\sigma$ , and  $c_{k\sigma}$  ( $c_{k\sigma}^\dagger$ ) is their annihilation (generation) operator in momentum representation. Here and in the following we have set physical quantities  $\hbar = k_B = 1$  for convenience. The interaction  $g_{1D} = -\gamma n_0/m$  describes an attractive interplay between opposite spin components with a dimensionless quantity  $\gamma$ . Since we consider a uniform system with bulk density  $n_0$ , the inverse of Fermi wave vector  $k_F = \pi n_0/2$  and Fermi energy  $E_F = k_F^2/2m$  are used as length and energy units, respectively. Usually the difference of chemical potential is used to define an effective Zeeman field  $h = (\mu_\uparrow - \mu_\downarrow)/2$ , and  $\mu = (\mu_\uparrow + \mu_\downarrow)/2$  is the average chemical potential.

At zero temperature  $T = 0$ , usually the system will come into a superfluid state, in which two opposite-spin atoms form a molecular Cooper pair to decrease energy. Interestingly, an FF-type superfluid, who has a non-zero COM momentum in Cooper pair, possibly turns out and even becomes the ground state at a non-zero effective Zeeman field  $h$ . In a standard mean-field treatment, the order parameter of FF superfluid can be expressed in a plane-wave form  $\Delta(x) \equiv \Delta e^{ipx}$ , where COM momentum  $p$  and pairing gap  $\Delta = g_{1D} \sum_k \langle c_{-k+p/2\downarrow} c_{k+p/2\uparrow} \rangle$  are two important degrees of freedom of order parameter  $\Delta(x)$ . Within this approximation, a mean-field Hamiltonian is expressed as

$$H_{\text{mf}} = \sum_k (\xi_k - h\sigma_z) c_{k\sigma}^\dagger c_{k\sigma} - \Delta^2/g_{1D} - \sum_k \Delta (c_{-k+p/2\downarrow} c_{k+p/2\uparrow} + h.c.), \quad (2)$$

where  $\xi_k = \epsilon_k - \mu$ . The exact solution of mean-field Hamiltonian  $H_{\text{mf}}$  can be obtained by motion equation of Green's functions. Finally we get three Green's functions, whose expressions are listed below

$$G_1 \equiv \langle\langle c_{k+p/2\uparrow} | c_{k+p/2\uparrow}^\dagger \rangle\rangle = \sum_l \frac{[G_1]_k^l}{\omega - E_k^l}, \quad (3)$$

$$G_{2R} \equiv \langle\langle c_{-k+p/2\downarrow}^\dagger | c_{-k+p/2\downarrow} \rangle\rangle = \sum_l \frac{[G_{2R}]_k^l}{\omega - E_k^l}, \quad (4)$$

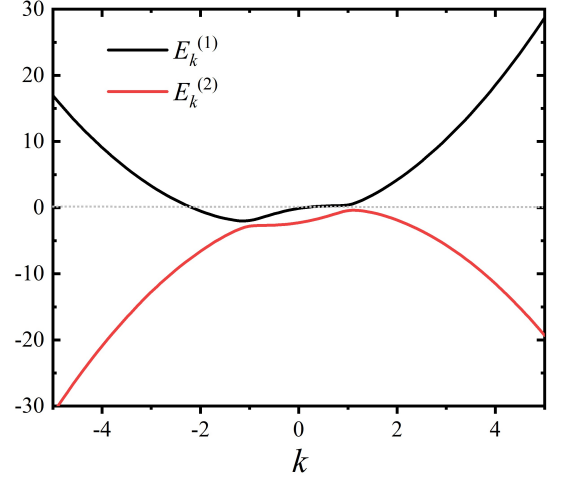


Figure 1. Two branches of single-particle excitation spectrum at interaction strength  $\gamma = 3$  and effective Zeeman field  $h = 1.2E_F$ . Here COM momentum  $p = 1.18k_F$ .

$$\Gamma \equiv \langle\langle c_{k+p/2\uparrow} | c_{-k+p/2\downarrow} \rangle\rangle = \sum_l \frac{[\Gamma]_k^l}{\omega - E_k^l}, \quad (5)$$

The double brackets in above equations are used to define Fourier transformation of double-time Green's function. Here it should be emphasized that the expression of spin-down Green's functions  $G_{2R}$  is different from the one of spin-up Green's function  $G_1$ . Their definitions closely depend on their way coupled to pairing Green's function  $\Gamma$  when solving motion equation of Green's function. All expressions related to  $[G_1]_k^l$ ,  $[G_{2R}]_k^l$  and  $[\Gamma]_k^l$  will be listed in the last appendix.  $l = 1, 2$  denotes two branches of quasi-particle energy spectrum  $E_k^{(1)}$  and  $E_k^{(2)}$ ,

$$E_k^{(1,2)} = \frac{kp}{2m} - h \pm E_k, \quad (6)$$

where  $E_k = \sqrt{\xi_{kp}^2 + \Delta^2}$  and  $\xi_{kp} = \epsilon_k + \epsilon_p/4 - \mu$ . In typical parameters used in this paper, we find that the value of  $E_k^{(2)}$  is always negative, while  $E_k^{(1)}$  can be either positive or negative. The distributions of these two spectra are shown in Fig. 1, in which  $E_k^{(1)}$  is negative when  $-2.17k_F < k < 0.12k_F$ .

The mean-field thermodynamic potential of the system reads

$$\Omega = -\Delta^2/g_{1D} + \sum_k (\xi_k - E_k) + \sum_k T \left[ \ln f(-E_k^{(1)}) + \ln f(E_k^{(2)}) \right], \quad (7)$$

which is connected to the free energy by  $F = \Omega + \mu N$ . Here  $f(x) = 1/(e^{x/T} + 1)$  is the Fermi-Dirac distribution function at temperature  $T$ . In this paper, we focus our discussion on an almost zero temperature ( $T = 0.01T_F$ ), to avoid an unnecessary numerical divergence induced by zeros of  $E_k^{(1)}$ .

## B. State of equations

The values for average chemical potential  $\mu$ , amplitude of order parameter  $\Delta$  and COM momentum  $p$  can be respectively determined with minimization of thermodynamic potential  $\Omega$  in Eq. 7 to them, namely  $N = -\partial\Omega/\partial\mu$ ,  $\partial\Omega/\partial\Delta = 0$  and  $\partial\Omega/\partial p = 0$ . These three relations respectively give the total particle number equation

$$N = \sum_k \left(1 - \frac{\xi_{kp}}{E_k}\right) + \sum_k \frac{\xi_{kp}}{E_k} \left[ f(E_k^{(1)}) + f(-E_k^{(2)}) \right], \quad (8)$$

pairing gap equation

$$\frac{\Delta}{g_{1D}} = \sum_k \frac{\Delta}{2E_k} \left[ f(E_k^{(1)}) + f(-E_k^{(2)}) - 1 \right], \quad (9)$$

and COM momentum equation

$$\sum_k \left[ p \left(1 - \frac{\xi_{kp}}{E_k}\right) + \left(2k + \frac{\xi_{kp}}{E_k} p\right) f(E_k^{(1)}) - \left(2k - \frac{\xi_{kp}}{E_k} p\right) f(-E_k^{(2)}) \right] = 0. \quad (10)$$

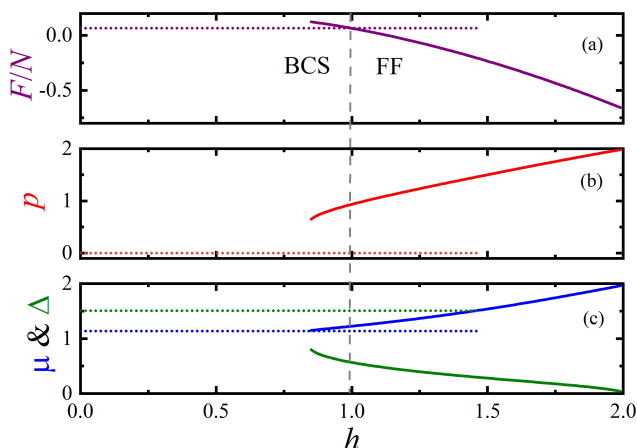


Figure 2. State of equation at interaction strength  $\gamma = 3$ . Three panels show the curves of (a) free energy, (b) COM momentum and (c) average chemical potential and order parameter at different effective Zeeman field, respectively.

The value of  $\mu$ ,  $\Delta$  and  $p$  should be self-consistently solved with Eqs. 8, 9 and 10.

The possible stable state of a system is determined by all minima in free energy  $F$ . Generally there are three possible states here. Besides the trivial normal state, who always has a zero pairing gap  $\Delta$  and the largest free energy, the conventional BCS superfluid and FF superfluid are the other two states with relatively lower free energy. As shown in Fig. 2, at a small  $h$ , the conventional BCS superfluid is the ground state of the system, whose COM momentum  $p = 0$ . The value of  $h$  can hardly influence the chemical potential  $\mu$  and pairing gap  $\Delta$ , which can be thought as the analogy of the Meissner effect in the superfluid. Interestingly an FF superfluid with a non-zero COM momentum  $p$  begins to turn out when  $h$  is large enough, whose free energy is larger than the one of BCS

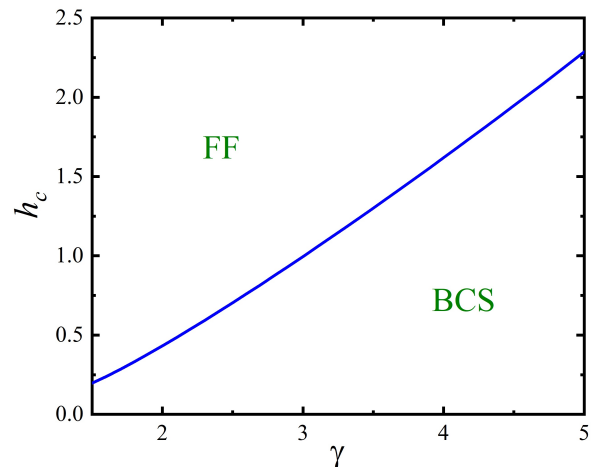


Figure 3. The critical effective Zeeman field  $h_c$  at different interaction strength  $\gamma$ .

superfluid. When  $h$  comes to a critical value  $h_c$  (a little smaller than  $1.0E_F$  here), this FF superfluid shares the same free energy as BCS superfluid. Further increasing  $h$ , FF superfluid will replace BCS superfluid to be the new ground state of the system for  $h > h_c$ . This phase transition had been introduced in Ref. [15]. Here  $\Delta$  and  $p$  are two necessary degree of freedom of in a FF-type order parameter  $\Delta(x) = \Delta e^{ipx}$ . Pairing gap  $\Delta$  is related to the conventional gauge symmetry breaking between normal state and superfluidity, and the direction of COM momentum  $p$  is related to another spontaneous symmetry breaking since  $\pm p$  corresponding the same free energy. While  $\Delta$  always decreasing with  $h$ ,  $p$  shows a monotonically increasing behaviour with  $h$ . The different dependence behavior of  $\Delta$  and  $p$  with effective Zeeman field  $h$  goes on reflecting that they come from different symmetry breaking and may induce different collective modes.

It is easy to know that the phase transition shown in Fig. 2 is a first-order one, which is manifested by the discontinuous behavior of  $\mu$ ,  $\Delta$  and  $p$ . We have checked that the same phase transition also happens at different interaction strength  $\gamma$  with different critical Zeeman field strength  $h_c$ , whose value is shown in Fig. 3. A larger interaction strength  $\gamma$  requires a bigger critical effective Zeeman field  $h_c$  to make the system come into the FF superfluid state.

### C. Calculation of dynamical excitations

When an interacting system comes into a superfluid state, usually there will be four typical densities. Besides the normal spin-up density  $n_1 = \langle \psi_{\uparrow}^{\dagger} \psi_{\uparrow} \rangle$  and spin-down density  $n_2 = \langle \psi_{\downarrow}^{\dagger} \psi_{\downarrow} \rangle$ , the pairing physics of opposite-spin atoms generates the other anomalous density  $n_3 = \langle \psi_{\downarrow} \psi_{\uparrow} \rangle$  and its conjugate counterpart  $n_4 = \langle \psi_{\uparrow}^{\dagger} \psi_{\downarrow}^{\dagger} \rangle$ . These pairs form phase coherent Cooper pairs with zero or finite COM momentum  $p$ . The interaction between particles makes these four densities couple closely with each other. Any fluctuation in each kind of density will influence other densities and generate an obvious density fluctuation of them. Also any weak perturbation potential  $V_{\text{pert}}$  will generate density fluctuations  $\delta n$ , and they are connected with each other by response function  $\chi$ , namely  $\delta n = \chi V_{\text{pert}}$ , in the frame of linear response theory.

The entire dynamical excitations of the system consist of possible collective excitations and single-particle excitations, which are also mainly connected to the physical properties of Cooper pairs. The phase spontaneously breaking of them generates a gapless Goldstone collective mode, while the breaking of Cooper pairs forming parts of single-particle excitation. These dynamical excitations can be well described by the density dynamic structure factor, which is from the imaginary part of related response functions  $\chi$ . The direct calculation of dynamic structure factor suffers from the many-body difficulty. A potential approximation to overcome this problem is the random phase approximation, which is firstly brought by P. W. Anderson and has been verified to be a qualitatively reliable way to study dynamical excitations. In our previous work, we had introduced how to calculate dynamic structure factor with random phase approximation [31, 32]. This approximation finds the connection between the beyond mean-field response function  $\chi$  and its mean-field approximation  $\chi^0$ , whose calculation is relatively easier, by the following equation

$$\chi = \frac{\chi^0}{1 - \chi^0 M_I g_{1D}}, \quad (11)$$

where the constant matrix  $M_I = \sigma_0 \otimes \sigma_x$  is the direct product of unit matrix  $\sigma_0$  and Pauli matrix  $\sigma_x$ , reflecting the coupling situation of four types of densities.  $\chi^0$

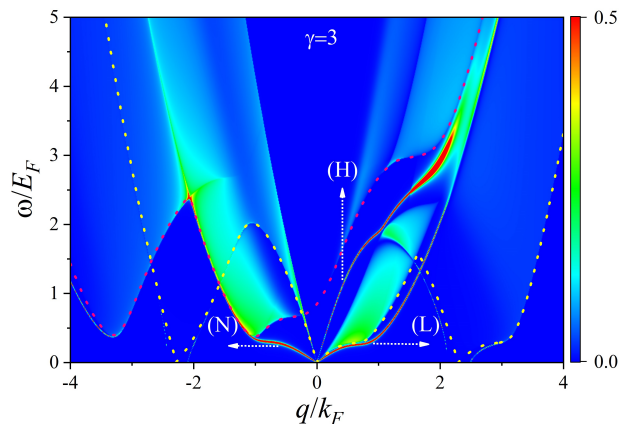


Figure 4. The density dynamic structure factor  $S_n(q, \omega)$  of FF superfluid at interacting strength  $\gamma = 3$ . (L) the lower collective phonon mode along the COM momentum  $p$  direction, (H) the higher collective phonon mode, (N) the collective phonon mode in the opposite direction of  $p$ .

is a four dimension matrix in mean-field level, and its  $ij$  matrix element  $\chi_{ij}^0$  reflects the interaction-induced coupling between density  $n_i$  and  $n_j$ . When the system comes into the FF superfluid,  $\chi^0$  has nine independent matrix elements, namely

$$\chi^0 = \begin{bmatrix} \chi_{11}^0 & \chi_{12}^0 & \chi_{13}^0 & \chi_{14}^0 \\ \chi_{12}^0 & \chi_{22}^0 & \chi_{23}^0 & \chi_{24}^0 \\ \chi_{14}^0 & \chi_{24}^0 & -\chi_{12}^0 & \chi_{34}^0 \\ \chi_{13}^0 & \chi_{23}^0 & \chi_{43}^0 & -\chi_{12}^0 \end{bmatrix}. \quad (12)$$

After Fourier transformation to above response function, we obtain the expression of all matrix elements in the momentum-energy representation.

With Eqs. 11 and 12, we can obtain the expression of total-density response function  $\chi_n \equiv \chi_{11} + \chi_{22} + \chi_{12} + \chi_{21}$ . Based on the fluctuation and dissipation theorem, its imaginal part is connected to density dynamical structure factor by

$$S_n = -\frac{1}{\pi} \frac{1}{1 - e^{-\omega/T}} \text{Im}(\chi_n). \quad (13)$$

## III. RESULTS

We numerically calculate the density dynamic structure factor  $S_n(q, \omega)$  of an FF superfluid at interaction strength  $\gamma = 3$ . We define the direction of COM momentum  $p$  is along the positive direction of transferred momentum  $q$ . The results are shown in Fig. 4. Intuitively we see an anisotropic dynamical behavior. The dynamical excitation at a positive transferred momentum  $q$  is different from the one at a negative  $q$ . This is due to the direction dependence of the non-zero COM momentum  $p$  in FF superfluid. Along the direction of COM momentum  $p$  (namely  $q > 0$ ), we see two kinds of

gapless collective mode (curves marked by (L) and (H)), and two-separated regimes of single-particle excitation. When  $q < 0$ , the higher gapless collective mode disappears, and two kinds of single-particle excitations overlap with each other. The speed of gapless collective phonon mode (curve marked by (N)) is a little smaller than that in the positive direction. In the following, we will separately introduce collection modes and single-particle excitations.

### A. Collective excitation

The origin of collective mode is closely related to the symmetry breaking of a certain matter state. A gapless collective excitation comes from a certain spontaneous symmetry breaking of the system. It is interesting to notice that there are two gapless collective modes at a positive transferred momentum  $q$ , which are also displayed at Fig. 4. The lower mode is the conventional collective Goldstone phonon mode (marked by (L)), which requires the lowest excitation energy among all possible excitations. Its physical origin is due to the gauge symmetry breaking of the phase of order parameter  $\Delta(x)$ . The higher gapless collective mode (marked by (H)) is due to the symmetry breaking of the direction of COM momentum  $p$ , which is continuous symmetry breaking in higher dimension system but not continuous in 1D system due to its specific spatial dimension. A similar mode as the higher collective mode here is also reported in a LO-type superconductor with order parameter  $\Delta(x) = \Delta \cos(px)$ , which is called the gapless Higgs mode since its amplitude of order parameter displays spatial periodic variation. However, this should be different from the one in FF superfluid, whose amplitude is always a constant value to keep continuous translational symmetry. So the higher collective mode in FF superfluid we argue that it is better to be called a gapless phonon-like mode, instead of a gapless Higgs mode.

The other difference from the BCS superfluid is that the lowest collective phonon mode displays an anisotropic excitation between the positive and negative direction, which is due to the direction dependence of COM momentum  $p$  in FF superfluid. The similar anisotropic dynamics of phonon mode is also reported in a spin-polarized Fermi system in square optical lattice [30]. From Fig. 5, it is easy to know that the velocity of phonon mode in a negative  $p$  direction (marked by (N)) is always smaller than the one in the positive  $q$  direction. Also the absolute value of phonon velocity decreases with  $h$  in the negative  $q$  direction.

The effective Zeeman field  $h$ -dependence of the speed for three collective modes is shown in Fig. 5, which displays that both  $v_L$  and  $v_N$  decrease with  $h$  and slowly goes to zero at a large enough  $h$ . Finally  $\Delta$  also touch zero and the superfluid disappears when  $h$  is around  $2.0E_F$ . However,  $v_H$  always rises with  $h$ , and this behavior is consistent with that of COM momentum  $p$  (panel

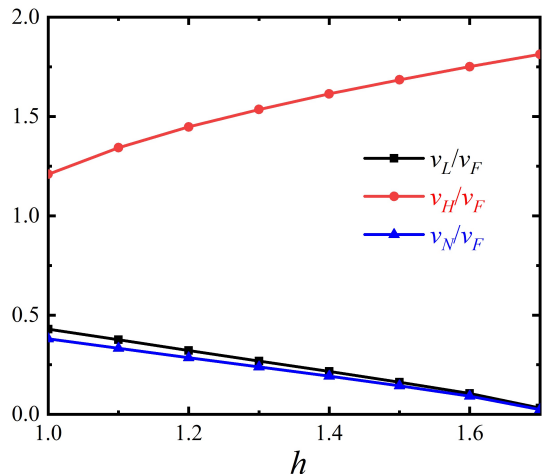


Figure 5. Speeds of three collective modes at different effective Zeeman field  $h$ .  $v_L$  and  $v_H$  are respectively the speed of lower and higher branch collective mode along the direction of COM momentum  $p$ , while  $v_N$  is the speed of collective mode in the opposite direction of  $p$ .

(b) in Fig. 2). The similar  $h$ -dependence between  $v_H$  and  $p$  again demonstrates a close connection between them. Also the different  $h$ -dependence between  $v_L$  and  $v_N$  demonstrates that the two gapless collective modes come from different symmetry breaking mechanism, and are related to different fluctuation of order parameter.

### B. Single-particle excitation

Now we discuss the pair-breaking excitation, which is an important part of single-particle excitation and takes up large regimes in Fig. 4. This excitation is usually a continuous excitation and its lowest excitation energy is determined by the single-particle spectrum (Eq. 6). To understand all possible ways of pair-breaking excitation, it is better to understand this physics by part of expression in response function  $\chi^0$ , namely

$$\frac{f(E_p^l) - f(E_{p+q}^{l'})}{i\omega_n + E_p^l - E_{p+q}^{l'}}. \quad (14)$$

Here  $E_p^l$  should consider all possible combinations of single-particle spectrum. As shown in Fig. 1,  $E_k^{(2)}$  is always negative, and  $E_k^{(1)}$  is positive except in a narrow regime  $-2.17k_F < k < 0.12k_F$ . The possible pair-breaking excitation may happen requiring that the numerator of Eq. 14 can not be zero, and also  $E_p^l - E_{p+q}^{l'} < 0$  to ensure a positive excitation energy.

Finally we find two possible pair-breaking excitations, namely  $|E_k^{(1)} - E_{k+q}^{(1)}|$  (11-type excitation) at a limited

regime of momentum  $k$  and  $|E_k^{(2)} - E_{k+q}^{(1)}|$  (21-type excitation) at a full regime of  $k$ . And their minima is the lowest energy to break an FF-type Cooper pair, which are labeled by both pink and yellow dotted lines in Fig. 4, respectively. It should be emphasized that the 11-type excitations (dotted yellow line) is a gapless pair-breaking excitation and is absent in the conventional BCS superfluid. Honestly there is a slight bias between predictions from yellow dotted lines and random phase approximation's prediction when  $q$  is around  $\pm 2.5k_F$ , which may be due to the limited excitation regime of momentum  $k$  in 11-excitation. The minimum of 21-type excitation is labeled with a dotted pink line. For a positive transferred momentum  $q$ , these two pair-breaking excitations are separated with each other by just the higher gapless collective mode. However, they are mixed with each other in a negative transferred momentum  $q$ . These differences can do help to find the higher collective mode in future experiment, and distinguish FF-type superfluid from BCS superfluid.

#### IV. CONCLUSIONS AND OUTLOOK

In summary, we theoretically calculate the dynamic structure factor of a 1D FF superfluid with random phase approximation to study dynamical excitations of the system. We find an anisotropic dynamical excitation between positive and negative directions in both collective modes and single-particle excitations. In the positive direction, we find two gapless collective modes. The lower one comes from the spontaneous breaking of gauge symmetry, while the higher one comes from the direction symmetry breaking of COM momentum  $p$ . The sound speed in the positive direction is larger than the one in the negative direction. There are two types of pair-breaking excitations, and one of them is a gapless excitation, which is absent in the BCS superfluid. In the positive direction, these two kinds of pair-breaking excitations are just separated by the higher gapless collective mode, but overlap with each other in the negative direction. These dynamical excitations can do help to distinguish FF superfluid from the conventional BCS superfluid in future experiment.

#### V. ACKNOWLEDGEMENTS

We are grateful for discussions with Wei Yi, Xiaoquan Yu and Hui Hu. This research was supported by National Natural Science Foundation of China under Grants No. 11804177 (P.Z.), No. 11547034 (H.Z.), Grant No. 11974384 (S.-G.P.) and 12374250 (S.-G.P.), and the National Key R&D Program under Grant No. 2022YFA1404102 (S.-G.P.).

#### VI. APPENDIX

In this appendix, we list expressions of three Green's functions and mean-field response function  $\chi^0$ . The first Green's function is  $G_1(k, \omega) = \sum_l [G_1]_k^l / (\omega - E_k^l)$ , with

$$[G_1]_k^{(1)} = \frac{E_k^{(1)} + \xi_{k-p/2+h}}{E_k^{(1)} - E_k^{(2)}}, \quad [G_1]_k^{(2)} = -\frac{E_k^{(2)} + \xi_{k-p/2+h}}{E_k^{(1)} - E_k^{(2)}}.$$

The second one is  $G_{2R}(k, \omega) = \sum_l [G_{2R}]_k^l / (\omega - E_k^l)$ , with

$$[G_{2R}]_k^{(1)} = \frac{E_k^{(1)} - \xi_{k+p/2+h}}{E_k^{(1)} - E_k^{(2)}}, \quad [G_{2R}]_k^{(2)} = -\frac{E_k^{(2)} - \xi_{k+p/2+h}}{E_k^{(1)} - E_k^{(2)}}.$$

The third Green's function is  $\Gamma(k, \omega) = \sum_l [\Gamma]_k^l / (\omega - E_k^l)$ , with

$$[\Gamma]_k^{(1)} = -\frac{\Delta}{E_k^{(1)} - E_k^{(2)}}, \quad [\Gamma]_k^{(2)} = \frac{\Delta}{E_k^{(1)} - E_k^{(2)}}.$$

The expressions of all nine independent matrix elements in mean-field response function  $\chi^0$  are respectively

$$\begin{aligned} \chi_{11}^0 &= + \sum_{pll'} [G_1]_p^l [G_1]_{p+q}^{l'} \frac{f(E_p^l) - f(E_{p+q}^{l'})}{i\omega_n + E_p^l - E_{p+q}^{l'}}, \\ \chi_{12}^0 &= - \sum_{pll'} [\Gamma]_p^l [\Gamma]_{p+q}^{l'} \frac{f(E_p^l) - f(E_{p+q}^{l'})}{i\omega_n + E_p^l - E_{p+q}^{l'}}, \\ \chi_{13}^0 &= + \sum_{pll'} [G_1]_p^l [\Gamma]_{p+q}^{l'} \frac{f(E_p^l) - f(E_{p+q}^{l'})}{i\omega_n + E_p^l - E_{p+q}^{l'}}, \\ \chi_{14}^0 &= + \sum_{pll'} [\Gamma]_p^l [G_1]_{p+q}^{l'} \frac{f(E_p^l) - f(E_{p+q}^{l'})}{i\omega_n + E_p^l - E_{p+q}^{l'}}, \\ \chi_{22}^0 &= + \sum_{kll'} [G_{2R}]_k^l [G_{2R}]_{k+q}^{l'} \frac{f(E_k^l) - f(E_{k+q}^{l'})}{i\omega_n + E_k^l - E_{k+q}^{l'}}, \\ \chi_{23}^0 &= - \sum_{kll'} [\Gamma]_k^l [G_{2R}]_{k+q}^{l'} \frac{f(E_k^l) - f(E_{k+q}^{l'})}{i\omega_n + E_k^l - E_{k+q}^{l'}}, \\ \chi_{24}^0 &= - \sum_{kll'} [G_{2R}]_k^l [\Gamma]_{k+q}^{l'} \frac{f(E_k^l) - f(E_{k+q}^{l'})}{i\omega_n + E_k^l - E_{k+q}^{l'}}, \\ \chi_{34}^0 &= + \sum_{kll'} [G_{2R}]_k^l [G_1]_{k+q}^{l'} \frac{f(E_k^l) - f(E_{k+q}^{l'})}{i\omega_n + E_k^l - E_{k+q}^{l'}}, \\ \chi_{43}^0 &= + \sum_{kll'} [G_1]_k^l [G_{2R}]_{k+q}^{l'} \frac{f(E_k^l) - f(E_{k+q}^{l'})}{i\omega_n + E_k^l - E_{k+q}^{l'}}. \end{aligned}$$

[1] P. Fulde and R. A. Ferrell, *Superconductivity in a Strong Spin-Exchange Field*, *Phys. Rev.* **135**, A550 (1964).

[2] A. I. Larkin and Y. N. Ovchinnikov, *Inhomogeneous state of superconductors*, *Zh. Eksp. Teor. Fiz.* **47**, 1136 (1964);

- [Sov. Phys. JETP **20**, 762 (1965)].
- [3] For reviews on the FFLO states, see, for examples, R. Casalbuoni and G. Nardulli, *Inhomogeneous superconductivity in condensed matter and QCD*, *Rev. Mod. Phys.* **76**, 263 (2004); J. J. Kinnunen, J. E. Baarsma, J.-P. Martikainen and P. Törmä, *The Fulde-Ferrell-Larkin-Ovchinnikov state for ultracold fermions in lattice and harmonic potentials: a review*, *Rep. Prog. Phys.* **81**, 046401 (2018).
- [4] Y. Matsuda and H. Shimahara, *Fulde-Ferrell-Larkin-Ovchinnikov State in Heavy Fermion Superconductors*, *J. Phys. Soc. Jpn.* **76**, 051005 (2007).
- [5] H. A. Radovan, N. A. Fortune, T. P. Murphy, S. T. Hannahs, E. C. Palm, S. W. Tozer, and D. Hall, *Magnetic enhancement of superconductivity from electron spin domains*, *Nature* **425**, 51 (2003).
- [6] K. Gloos, R. Modler, H. Schimanski, C. D. Bredl, C. Geibel, F. Steglich, A. I. Buzdin, N. Sato, and T. Komatsubara, *Possible formation of a nonuniform superconducting state in the heavy-fermion compound UPd<sub>2</sub>Al<sub>3</sub>*, *Phys. Rev. Lett.* **70**, 501 (1993).
- [7] A. D. Huxley, C. Paulson, O. Laborde, J. L. Tholence, D. Sanchez, A. Junod, and R. Calemczuk, *Flux pinning, specific heat and magnetic properties of the laves phase superconductor CeRu<sub>2</sub>*, *J. Phys.: Condens. Matter* **5**, 7709 (1993).
- [8] A. Bianchi, R. Movshovich, C. Capan, P. G. Pagliuso, and J. L. Sarrao, *Possible Fulde-Ferrell-Larkin-Ovchinnikov Superconducting State in CeCoIn<sub>5</sub>*, *Phys. Rev. Lett.* **91**, 187004 (2003).
- [9] C. Martin, C. C. Agosta, S. W. Tozer, H. A. Radovan, E. C. Palm, T. P. Murphy, and J. L. Sarrao, *Evidence for the Fulde-Ferrell-Larkin-Ovchinnikov state in CeCoIn<sub>5</sub> from penetration depth measurements*, *Phys. Rev. B* **71**, 020503(R) (2005).
- [10] M. Croitoru and A. Buzdin, *In search of unambiguous evidence of the Fulde-Ferrell-Larkin-Ovchinnikov state in quasi-low-dimensional superconductors*, *Condens. Matter* **2**, 30 (2017).
- [11] Y. Liu, T. Wei, G. He, Y. Zhang, Z. Wang & J. Wang, *Pair density wave state in a monolayer high-Tc iron-based superconductor*, *Nature* **618**, 934 (2023).
- [12] H. Zhao, R. Blackwell, M. Thinel, T. Handa, S. Ishida, X. Zhu, A. Iyo, H. Eisaki, A. N. Pasupathy & K. Fujita, *Smectic pair-density-wave order in EuRbFe<sub>4</sub>As<sub>4</sub>*, *Nature* **618**, 940 (2023).
- [13] A. Aishwarya, J. M.-Mann, A. Raghavan, L. Nie, M. Romanelli, S. Ran, S. R. Saha, J. Paglione, N. P. Butch, E. Fradkin & V. Madhavan, *Magnetic-field-sensitive charge density waves in the superconductor UTe<sub>2</sub>*, *Nature* **618**, 928 (2023).
- [14] L. Radzihovsky and D. E. Sheehy, *Imbalanced Feshbach-resonant Fermi gases*, *Rep. Prog. Phys.* **73**, 076501 (2010).
- [15] X.-J. Liu, H. Hu, and P. D. Drummond, *Fulde-Ferrell-Larkin-Ovchinnikov states in one-dimensional spin-polarized ultracold atomic Fermi gases*, *Phys. Rev. A* **76**, 043605 (2007).
- [16] H. Hu and X.-J. Liu, *Fulde-Ferrell superfluidity in ultracold Fermi gases with Rashba spin-orbit coupling*, *New J. Phys.* **15**, 093037 (2013).
- [17] X.-J. Liu and H. Hu, *Inhomogeneous Fulde-Ferrell superfluidity in spin-orbit-coupled atomic Fermi gases*, *Phys. Rev. A* **87**, 051608(R) (2013).
- [18] L. He, H. Hu, and X.-J. Liu, *Realizing Fulde-Ferrell Superfluids via a Dark-State Control of Feshbach Resonances*, *Phys. Rev. Lett.* **120**, 045302 (2018).
- [19] I. Bloch, J. Dalibard, and W. Zwerger, *Many-body physics with ultracold gases*, *Rev. Mod. Phys.* **80**, 885 (2008).
- [20] S. Giorgini, L.P. Pitaevskii, S. Stringari, *Theory of ultracold atomic Fermi gases*. *Rev. Mod. Phys.* **80**, 1215 (2008).
- [21] G. Veeravalli, E. Kuhnle, P. Dyke, and C. J. Vale, *Bragg Spectroscopy of a Strongly Interacting Fermi Gas*, *Phys. Rev. Lett.* **101**, 250403 (2008).
- [22] S. Hoink, P. Dyke, M. G. Lingham, J. J. Kinnunen, G. M. Bruun and C. J. Vale, *Goldstone mode and pair-breaking excitations in atomic Fermi superfluid*, *Nat. Phys.* **13**, 943 (2017).
- [23] X. Li, X. Luo, S. Wang, K. Xie, X.-P. Liu, H. Hu, Y.-A. Chen, X.-C. Yao, J.-W. Pan, *Second sound attenuation near quantum criticality*, *Science* **375**, 528 (2022).
- [24] P. Dyke, S. Musolino, H. Kurkjian, D. J. M. Ahmed-Braun, A. Pennings, I. Herrera, S. Hoinka, S. J. J. M. F. Kokkelmans, V. E. Colussi, and C. J. Vale, *Higgs oscillations in a unitary Fermi superfluid*, [arXiv:2310.03452v1](https://arxiv.org/abs/2310.03452v1).
- [25] R. Senaratne, D. C.-Cavazos, S. Wang, F. He, Y.-T. Chang, A. Kafle, H. Pu, X.-W. Guan, R. G. Hulet, *Spin-charge separation in a one-dimensional Fermi gas with tunable interactions*, *Science* **376**, 1305 (2022).
- [26] P. W. Anderson, *Random-phase approximation in the superconductivity*, *Phys. Rev.* **112**, 1900 (1958).
- [27] X.-J. Liu, H. Hu, A. Minguzzi, and M. P. Tosi, *Collective oscillations of a confined Bose gas at finite temperature in the random-phase approximation*, *Phys. Rev. A* **69**, 043605 (2004).
- [28] K. V. Samokhin, *Goldstone modes in Larkin-Ovchinnikov-Fulde-Ferrell superconductors*, *Phys. Rev. B* **81**, 224507 (2010).
- [29] Z. Huang, C. S. Ting, J.-X. Zhu, and S.-Z. Lin, *Gapless Higgs mode in the Fulde-Ferrell-Larkin-Ovchinnikov state of a superconductor*, *Phys. Rev. B* **105**, 014502 (2022).
- [30] M. O. J. Heikkinen and P. Törmä, *Collective modes and the speed of sound in the Fulde-Ferrell-Larkin-Ovchinnikov state*, *Phys. Rev. A* **83**, 053630 (2011).
- [31] Z. Gao, L. He, H. Zhao, S.-G. Peng, and P. Zou, *Dynamic structure factor of one-dimensional Fermi superfluid with spin-orbit coupling*, *Phys. Rev. A* **107**, 013304 (2023).
- [32] H. Zhao, X. Yan, S.-G. Peng, and P. Zou, *Dynamic structure factor of two-dimensional Fermi superfluid with Rashba spin-orbit coupling*, *Phys. Rev. A* **108**, 033309 (2023).